Phosphoric Acid Treated Oil Palm Trunk Waste for Removal of Malachite Green – Kinetics and Isotherm Investigations

Zarifah Aisyah Zainon Abidin[1], Waheeba Ahmed Al-Amrani[2], Faiz Bukhari Mohd Suah[3], Shariff Ibrahim[4], Megat Ahmad Kamal Megat Hanafiah[1*]

[1] Faculty of Applied Sciences, Universiti Teknologi MARA Pahang, 26400, Jengka, Pahang, Malaysia

[2] Department of Chemistry, College of Science, Ibb University, Ibb, Yemen

[3] School of Chemical Sciences, Universiti Sains Malaysia, 11800, Minden, Penang, Malaysia

[4] Faculty of Applied Sciences, Universiti Teknologi MARA, 40450, Shah Alam, Selangor, Malaysia

* Corresponding author's e-mail: makmh@uitm.edu.my

ABSTRACT

Dyeing operations in industries like textiles, paper, and leather are significant contributors to environmental pollution due to the release of harmful dyes. The current study aimed to examine the use of oil palm trunk (OPT) treated with phosphoric acid (PAOPT) to remove malachite green (MG) dye from aqueous solutions through batch adsorption experiments. Spectroscopic and quantitative tests were used to characterise the PAOPT adsorbent. The effects of initial solution pH (3–6), PAOPT dosage (0.02–0.10 g), and adsorption duration (0–120 min) were studied. The adsorption rate of MG followed a pseudo-second-order kinetic model with a high regression correlation (R^2) and a low chi-squared value (χ^2). The single-layer adsorption of PAOPT for MG was determined to be 217.23 mg/g at a pH of 6, 0.02 g PAOPT mass, 20 min contact time, and 298 K. The percentage of MG desorption from the loaded PAOPT using distilled water and 0.01 M HCl was 0% and 19.65%, respectively, indicating the possible involvement of electrostatic interactions between the dye and PAOPT, π-π interaction and hydrogen bonding. The experimental results of the current study and the assessment with other stated adsorbents indicate that PAOPT could be used as a cost-effective alternative adsorbent for MG removal.

Keywords: adsorption, isotherm, kinetic, malachite green, oil palm trunk.

INTRODUCTION

The contamination of the environment is a worldwide issue, and the textile industry stands out as the largest contributor due to its excessive water usage. Despite even small amounts of dyes being detectable, the dyed water produced during fabric dyeing is likely the most severe form of pollution. Paper, pulp, dyes, distilleries, food, plastics, leather, cosmetics and tanneries also produce heavily coloured effluents [Pereira and Alves, 2012; Haroon et al., 2021]. Malachite green (MG) is used to dye leather, silk, cotton, wool, paper, jute, distilleries and more. In aquaculture, it is used as a fungicide, antiseptic and antiparasitic. Despite being prohibited, this dye is still utilised in several countries, primarily because of its affordability, accessibility, and effectiveness. Recent discoveries reveal that the oral consumption of this substance by animals can result in toxicity, carcinogenicity, mutagenicity, and teratogenicity [Gebreslassie, 2020; Jabar and Odusote, 2021]. Therefore, efficient technology is needed to treat dye wastewater before it can be discharged into natural waters.

Adsorption can separate a wide range of substances, is cost-effective, environmentally friendly and biocompatible, and can remove dyes from wastewater [Jabar and Odusote, 2021; Lan et al., 2022]. Adsorption technology began with the introduction of activated carbon [Ngaha et al., 2019]. However, activated carbon is

relatively expensive and difficult to regenerate after adsorption [Husien et al., 2022]. Therefore, several research projects have used bioresources such as lignocellulosic materials as alternative adsorbents that are cheap, locally available and efficient. Since then, various lignocellulosic materials have been explored for dye adsorption, all of which were able to remove dyes [N'diaye et al., 2022]. It has been discovered that the solid waste produced by oil palm industries is an efficient adsorbent for eliminating pollutants from the environment, notably harmful dyes [Lim et al., 2022; Ab Aziz et al., 2023].

The Malaysian palm oil industry produces 30 million tonnes of fronds, stems, empty fruit bunches and leaves annually. Because of poor waste management, the abundance of these wastes pollutes the ecosystem [Hasan et al., 2019]. Therefore, the use of oil palm waste to remove dyes from water is beneficial. In various studies on oil palm, anionic and cationic dyes have been removed from wastewater. The activated carbon (AC) extracted from oil palm trunks was able to remove sunset yellow (SY) and acid blue 25 (AB 25) [Lim et al., 2022] and indigo carmine (IC) in wastewater through cetyltrimethylammonium bromide-modified palm oil fibres [Ngaha et al., 2019]. A mesoporous AC of oil palm kernel shell (PKS) and oil palm frond (OPF) [Jasri et al., 2023], oil palm frond treated with eggshell (EG-OPF) [Hasan et al., 2019], alkali modified-OPT [Miranda et al., 2021; Mustikaningrum et al., 2021] and synthesised reduced graphene oxide (rGO) obtained from empty fruit fronds of oil palm (OPEFB) as a natural precursor [Ab Aziz et al., 2023] have been investigated to remove the cationic dye methylene blue [N'diaye et al., 2022]. However, oil palm as an adsorbent to remove the cationic dye MG has received less attention than MB. MG has been removed by AC of oil palm trunk fibre (OPTF) [Hameed and El-Khaiary, 2008], acid-treated OPF using a microwave-assisted method [Harith Zafrul Fazry et al., 2018] and date palm trunk fibre AC [Haroon et al., 2021]. However, there is no study on OPT treated with phosphoric acid to remove MG.

Thus, OPT was treated with phosphoric acid (PAOPT) and used in the current study to remove MG dye from wastewater. PAOPT was characterised by a Fourier transform infrared (FTIR) spectrophotometer, scanning electron microscope coupled with energy dispersive x-ray (SEM-EDX) microscope and pH of zero point charge or pH_{ZPC}.

The MG adsorption was investigated under different experimental conditions such as solution pH, PAOPT dosage and adsorption duration. The kinetics and equilibrium parameters were examined. The mechanisms involved in the MG adsorption process on adsorbents were also proposed.

MATERIALS AND METHODS

Preparation of OPT and PAOPT

The middle section of an oil palm trunk (OPT) aged > 25 years from a farm in Universiti Teknologi MARA Pahang, Jengka Campus, Malaysia, was employed as the natural adsorbent. The OPT was washed and heated at 60 °C for 72 h to remove moisture. The dry section was manually chopped into 0.5–1.0 cm pieces, crushed, and sieved to yield 0.5–1 mm particles. The sieved material was stored in an airtight plastic container. Then, 1.0 g of OPT particles was agitated for 2 h in 100 mL (0.10 M) of phosphoric acid (H_3PO_4) without heating, filtered and rinsed 10 times with 100 mL of distilled water (DW) and labelled as PAOPT. The PAOPT sample was dried at 80 °C for 2 h.
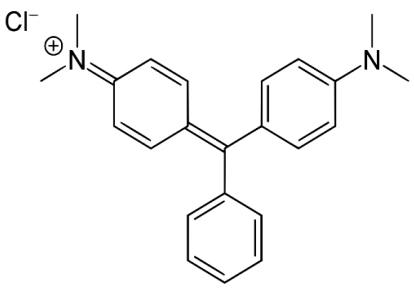
Preparation of adsorbate

The adsorption experiments were conducted utilising a water-based MG dye with 99% purity supplied by R&M Chemicals, Malaysia. A 1000 mg/L stock solution of MG dye was made by mixing it in distilled water (1 L), then diluted to obtain the chosen concentration of MG. Table 1 provides information about the molecular structure and properties of the MG dye. Analytical reagent-grade chemicals were employed throughout the study.

Characterisation of adsorbent

The surface functional groups of OPT, PAOPT and MG-loaded PAOPT were detected using an FTIR spectrophotometer (PerkinElmer, Spectrum 100, USA). The spectra were recorded from 4000 to 600 cm^{-1}. Also, OPT and PAOPT's surface morphology with MG-loaded PAOPT were examined using SEM coupled with EDX (Oxford Instrument, UK). The sample was deposited on a sample stub and sputtered with gold before analysis. The PAOPT was assessed for the surface charge using the pH_{ZPC} method as

Table 1. Characteristics of MG dye along with its molecular structure

Name of dye	Malachite green	Molecular structure
Type	Cationic dye	
Abbreviation	MG	
Chemical formula	$C_{23}H_{25}N_2Cl$	
Molecular weight	364.91 g/mol	
Common synonyms	Malachite green 569-64-2, China Green, Malachite green chloride Basic Green 4.	
Parent compound	CID 11295 (Malachite green cation)	
Appearance	Metallic lustre with green crystals Blue-green colour in water solution.	

follows: In conical flasks, 50 mL (0.01 M) NaCl solutions with starting pH (pH_i) values from 2 to 10 were equipped. A magnetic stirrer swirled 0.50 g of PAOPT in NaCl solutions for 24 h. After filtration, the supernatant's final pH (pH_f) was determined. The pH_{ZPC} of PAOPT was the curve that intersected the pH_i axis in the pH_i–pH_f versus pH_i plot.

Batch adsorption tests

Batch adsorption tests were conducted in 250 mL Erlenmeyer flasks with caps, agitated at 300 rpm using an orbital shaker (IKA RT 10 Power, Korea) using 50 mL of MG dye solution from the stock solution. In order to assess how the solution pH and amount of adsorbent affect PAOPT's

Table 2. Representation of the mathematical equations used in the MG dye adsorption process onto PAOPT adsorbent

No. Equation	Equation	Reference
1	$q_e = (C_o - C_e)\dfrac{V}{W}$	[Ab Aziz et al., 2023]
2	$Removal\ (\%) = \dfrac{C_o - C_e}{C_o} \times 100$	[Krishna Murthy et al., 2019]
3	$Desorption\ efficiency\ (\%) = \dfrac{\text{Total adsorption capacity after elution}}{\text{Total adsorption capacity after elution}} \times 100$	[Khalid et al., 2022]
4	$R^2 = \dfrac{\sum(q_{e,cal,i} - q_{e,exp,i})^2}{\sum(q_{e,cal,i} - q_{e,exp,avg})^2 - \sum(q_{e,cal,i} - q_{e,exp,i})^2}$	[Krishna Murthy et al., 2019]
5	$RSS = \sum(q_{exp,i} - q_{e,cal,i})^2$	
6	$X^2 = \sum_{i=1}^{N} \left| \dfrac{(q_{e,exp,i} - q_{e,cal,i})^2}{q_{e,exp,i}} \right|$	
7	$q_t = q_e(1 - e^{k_1 t})$	[Lagergren 1898]
8	$q_t = \dfrac{q_e^2 k_2 t}{(1 + k_2 q_e t)}$	[Ho and McKay, 1999]
9	$q_e = \dfrac{q_m K_L C_e}{1 + K_L C_e}$	[Langmuir, 1918]
10	$q_e = K_F C_e^{\frac{1}{n}}$	[Freundlich, 1926]

Note: q_e (mg/g) – the adsorption capacity at the equilibrium state, C_o and C_e (mg/L) – the liquid-phase dye concentrations at initial and equilibrium states, respectively, V (L) – the volume of the solution, W (g) – the mass of dry adsorbent used, q_t (mg/g) – the adsorption capacity of the dye at t (min), k_1 – the rate constant of pseudo-first-order adsorption (L/min), k_2 – the rate constant of pseudo-second-order adsorption (g/mg min), $q_{e,exp,i}$ and $q_{e,calc,i}$ – experimentally measured and model calculated adsorbate solid phase concentration on adsorbent at any observation i respectively, $q_{e,exp,avg}$ – average of experimentally measured observations, N – the number of observations, q_m (mg/g) – the maximum adsorption capacity, K_L (L/min) – the constant related to binding energy for adsorption, K_F (mg/g)/(mg/L)ⁿ – the Freundlich constant; n is the adsorption intensity parameter.

capacity to adsorb 20 mg/L of MG dye solution, the solution pH was altered between 3 and 6 while utilising a dosage of PAOPT ranging from 0.02 to 0.10 g for 120 min. The use of an alkali medium was avoided in this study as NaOH decolourised MG dye solution [Ahmad Khan et al., 2023]. Each experiment was pH-controlled by adding a few drops of 0.10 M NaOH or HCl using a pH meter (CyberScan, EUTECH Instruments pH 510, Singapore). For kinetic investigations, 0.02 g of PAOPT was combined with 50 mL of MG solutions at pH 6, with different initial MG concentrations of 5, 10, and 20 mg/L at different intervals. Batch isotherm equilibrium tests were done by adding 0.02 g of PAOPT into 50 mL of MG dye solution at pH 6 with varied beginning concentrations (40–200 mg/L) for 120 min. After equilibrium, MG concentrations were measured at 617 nm (λ_{max}) by a double-beam UV/Vis spectrophotometer (UV-1800, Shimadzu, Japan). The total of dye adsorbed and percentage of dye removal were reported using Equations 1 and 2, respectively, as shown in Table 2. Adsorption experiments were repeated twice, and the average findings were reported.

Desorption studies

Another environmental hazard could arise from the disposal of the exhausted loaded adsorbent. As a result, using pure water and 0.01 M HCl, this study evaluated the ability to desorb exhausted adsorbent at neutral and acidic pH. Initially, the PAOPT was loaded with MG dye as follows: At pH 6, 0.02 g of PAOPT was combined with 50 mL of 20 mg/L MG solution. The mixture was agitated at 300 rpm, 298 K, for 120 min. The mixture was subsequently filtered to separate the MG-loaded PAOPT, and the MG solution was spectroscopically analysed. The dried MG-loaded PAOPT was put into separate conical flasks (100 mL), and 50 mL of distilled water and 0.01 M HCl as eluents were added separately. The mixtures were agitated for 30 min at 298 K and 300 rpm. The mixture was subsequently filtered, and the MG desorbed was estimated using Equation 3, as shown in Table 2.

Statistical analysis

The non-linear regression analysis of the kinetics and isotherm models (kinetics and isotherm) employed in this study was done in Microsoft Excel using the Solver-add-in tool to fit the experimental data to specified models. In addition to the fundamental criterion of coefficient of determination (R^2), residual sum square (RSS) and non-linear chi-square (χ^2) were employed to evaluate the quality of fit. Statistical characteristics were calculated using the mathematical formulas (Equations 4–6 presented in Table 2).

RESULTS AND DISCUSSION

Characterisation of adsorbent

The FTIR spectra of untreated OPT, PAOPT, and MG-loaded PAOPT are shown in Figure 1. It can be noticed that the OPT spectrum has distinct peaks at 3335 cm^{-1}, which is often attributed to the existence of O-H groups stretching vibration. The broad peak from 2400 to 3600 cm^{-1} indicated the presence of the carboxylic acid group, particularly from the uronic acid [Abdul Khalil et al., 2008]. The weak peak at 3074 cm^{-1} suggests the -C=H group of the aromatic groups originated from lignin. Furthermore, the PAOPT spectrum contains fewer missing and new peaks than the OPT spectrum, showing that the carboxylic and ester connections of the raw OPT's hemicellulose and lignin structure were broken after phosphoric acid treatment. For example, the strong peak at 1673 cm^{-1} in OPT, which represents the carboxyl (-COO$^-$) group, diminished in PAOPT. The methoxy group of Klason lignin detected at 1290 cm^{-1} also diminished after treating OPT with H$_3$PO$_4$ acid. Furthermore, the peaks at 1602 cm^{-1} (for C = C stretching of the aromatic chain in lignin) and 1290 cm^{-1} (for Si-C stretching) disappeared from the PAOPT spectrum, while a new peak at 1731 cm^{-1} for carbonyl groups formed, showing the collapse of the lignin structure. The C-H stretching peak at 2832 cm^{-1} in the OPT spectrum was also detected in PAOPT (2899 cm^{-1}). The C-H bending was found at 1424 cm^{-1}, confirming the existence of cellulose in OPT.

After chemical alteration, the peak intensity at 1028 cm^{-1} for the -C-O-C- group in PAOPT became stronger [Hameed and El-Khaiary, 2008; Miranda et al., 2021]. These alterations provided a good hint for the successful chemical modification of OPT by phosphoric acid and confirmed that other functional groups, including carbonyl and hydroxyl groups, may be available in PAOPT adsorbent. After adsorption
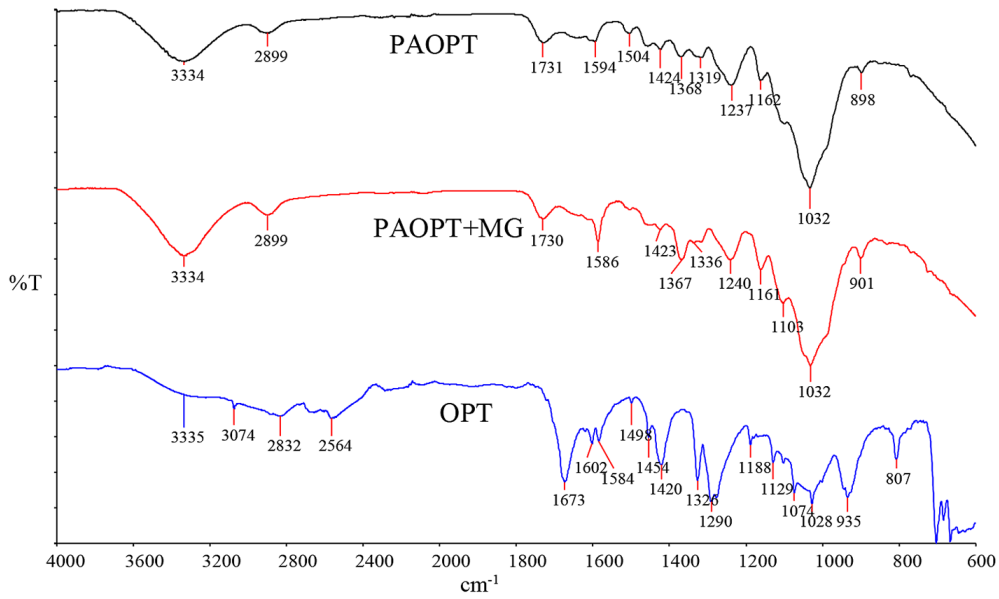
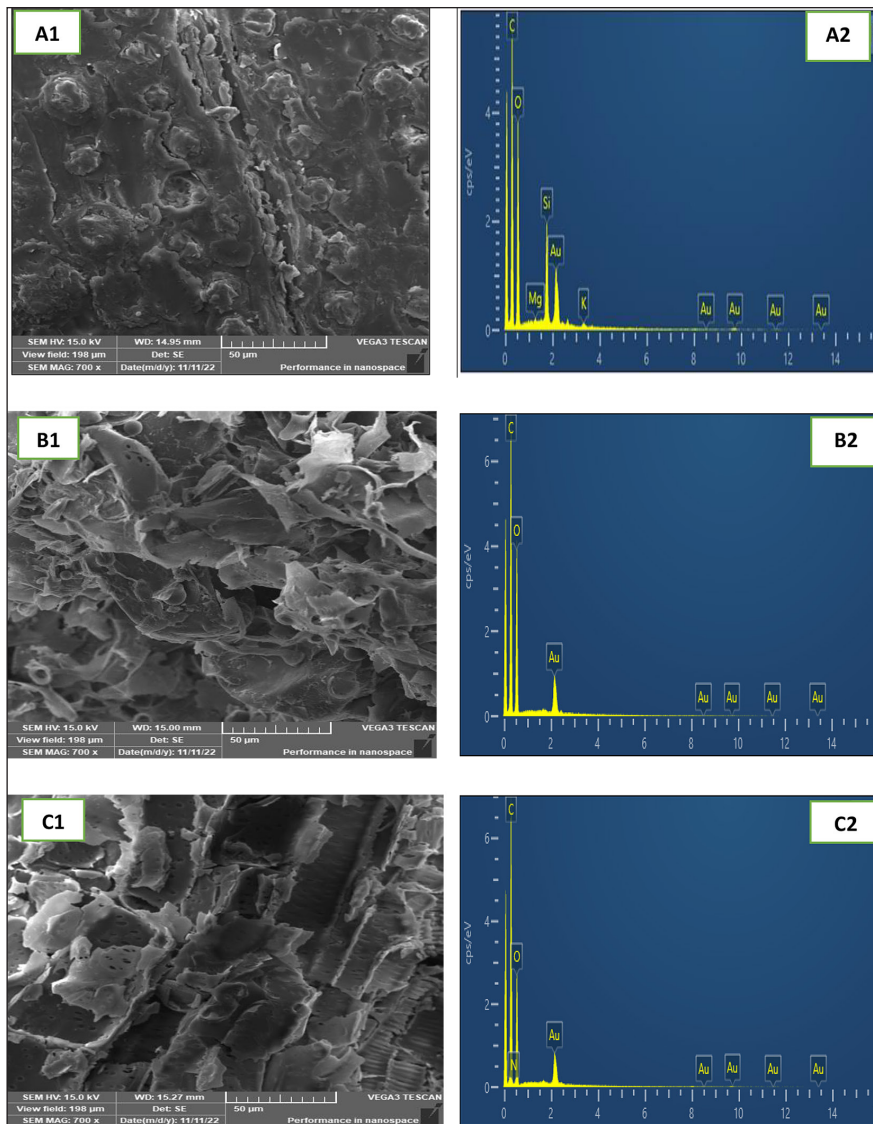**Figure 1.** FTIR spectra of untreated OPT, PAOPT and MG-loaded PAOPT

Figure 2. SEM (magnification = 700X) and EDX images of (A1–A2) OPT,
(B1–B2) PAOPT, and (C1–C2) MG-loaded PAOPT

with MG dye, a new peak at 1586 cm^{-1} was seen in the PAOPT for the NH$_2$ deformation group since MG dye contains N atoms in its chemical structure, as indicated in Table 1. Additionally, the increase in the intensity of the peaks at 3334 cm^{-1} and 1161 cm^{-1} corresponded to the N-H stretching vibration of primary amines and the C-N stretching bond, respectively, which confirms the MG adsorbed on PAOPT adsorbent [Harith Zafrul Fazry et al., 2018]. The intense/sharp peak indicated a strong contact between the OPT surface and the MG dye.

Figure 2 shows SEM (magnification 700 X) and EDX images of OPT, PAOPT, and MG-loaded PAOPT. Figure 2 (A1) shows the SEM cross-section of OPT, whereas Figure 2 (B1) shows PAOPT produced by the phosphoric acid treatment procedure. The surface textures of OPT were drastically different before and after the modification. Because of the presence of lignin and hemicellulose, the morphological appearance of OPT is noticeable in the cross-section to hard, caves-like, and uneven morphology surface, whereas PAOPT has a spongy with porous structure, indicating that H$_3$PO$_4$ damage to the OPT's cuticle results in a rise in interior surface area and also promotes the formation of pores. The residue also caused obvious damage to lignin and hemicellulose, resulting in a brighter residue, as seen in Figure 2 (B1). After adsorption, the surface of MG-loaded PAOPT demonstrates that it has been covered with a layer of MG dye, as proven by the N atom (Figure 2, C1).

Figure 2 (A2, B2, and C2) shows how EDX data from OPT, PAOPT, and MG-loaded PAOPT were used. The elements that are most plentiful in untreated OPT are carbon (C), oxygen (O), and silica (Si), with traces of magnesium (Mg) and potassium (K). However, as seen in Figure 2

(B2), PAOPT contains only carbon and oxygen, and the other elements were eliminated after the H$_3$PO$_4$ treatment for OPT alteration. Similarly, Figure 2 (C2) only shows carbon and oxygen, but the successful adsorption of MG dye on PAOPT resulted in a new peak for nitrogen (N).

The pH$_{ZPC}$ plot in Figure 3 has a value of 4.5. Adsorption of MG dye would be enhanced by a boost in the electrical attraction between the positively charged MG dye, and the negatively charged adsorbent (PAOPT) surface at a pH greater than pH$_{ZPC}$.

Effect of operational parameters

Influence of solution pH

The initial solution pH is crucial in the adsorption process since pH has a substantial influence on the surface features of the adsorbent in addition to the dye's molecular ionisation [Haroon et al., 2021; Lan et al., 2022]. Figure 4 depicts the influence of starting solution pH on MG adsorption onto PAOPT. The results show that the capability of MG dye adsorption was improved from 13.85 to 38.02 mg/g by increasing the pH from 3 to 6, respectively. This is explained by the fact that PAOPT has a zero-point charge of 4.5; thus, at pH > pH$_{ZPC}$, the hydroxyl ions concentration in the bulk solution increased, as a result of which the amount of negatively charged sites on the PAOPT surface has increased, which increased the electrostatic attraction among the cationic MG and the negatively charged sites on the PAOPT surface. Lower MG adsorption at acidic pH is caused by the competition of the abundant H$^+$ ions with dye cations for PAOPT adsorption positions. Several researchers have observed similar findings [Haroon et al., 2021; Ab Aziz et al., 2023].
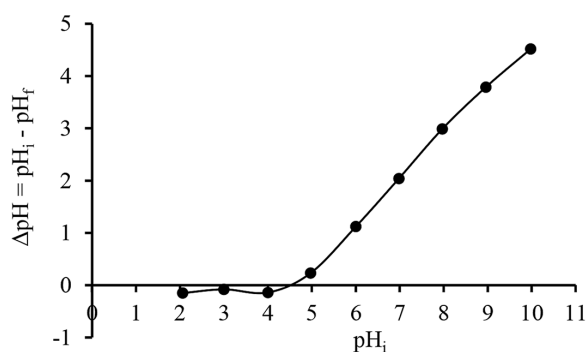
**Figure 3.** pH of zero-point charge (pH$_{ZPC}$) of PAOPT adsorbent
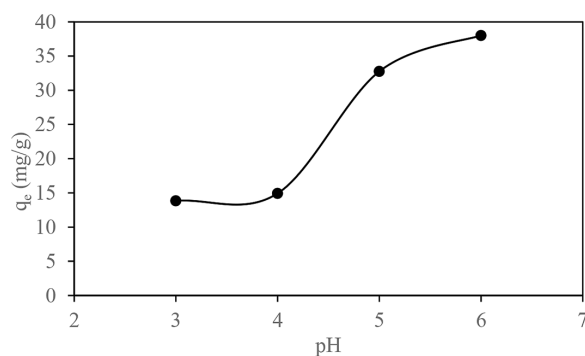
**Figure 4.** The effect of initial solution pH on the aqueous solution MG adsorption by PAOPT adsorbent

Influence of PAOPT dosage

Figure 5 depicts the influence of PAOPT dosage on MG adsorption. It can be seen that increasing the PAOPT dosage from 0.02 to 0.10 g increased the adsorption removal of MG in the bulk solution from 76.02 to 92.02% while decreasing the adsorption capacity of MG dye from 38.01 to 9.20 mg/g, respectively, at a constant dye concentration (20 ppm), pH 6, contact duration 120 min, and stirring speed of 300 rpm. The improvement in adsorption efficacy could be attributable to a rise in the accessible energetic locations for MG adsorption. The reduction in MG adsorption ability might be attributable to adsorption site overlapping or aggregation at higher adsorbent dosages, but the exposed surface area for adsorbate adsorption decreased. As a result, the following kinetics and isotherm studies were carried out with 0.02 g of PAOPT adsorbent. Similar adsorption studies yielded the same findings [Zaid et al., 2017; Ngaha et al., 2019].
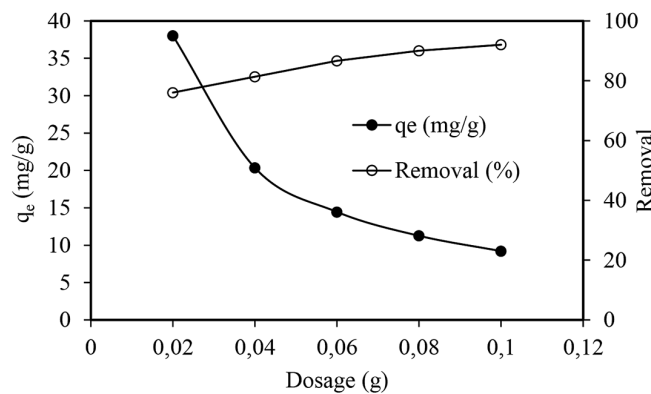
Figure 5. Effect of PAOPT dosage on the adsorption of MG dye
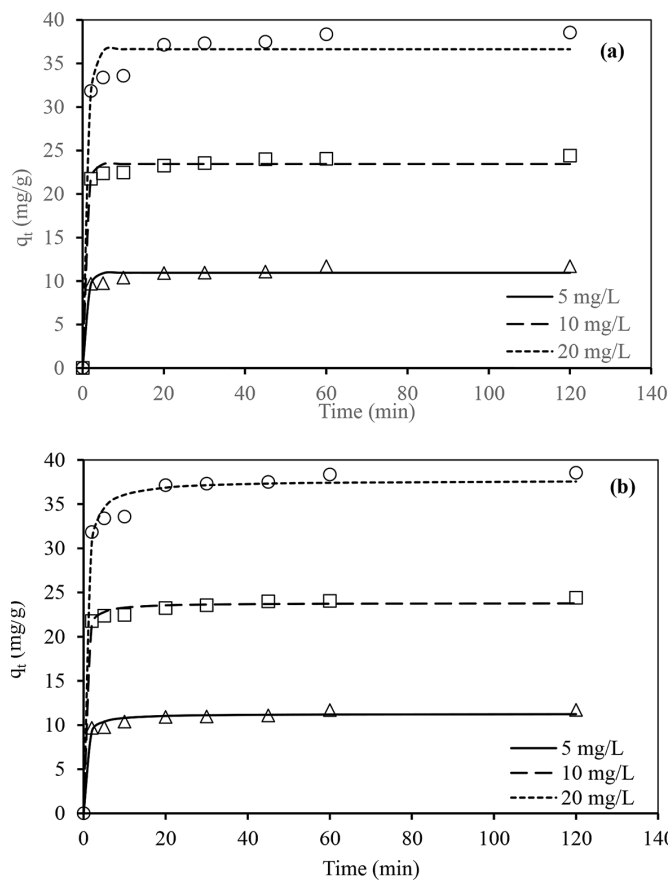
Figure 6. Non-linear fitting for adsorption kinetic models of (a) PFO and (b) PSO for the MG adsorption on PAOPT surface

Adsorption kinetic studies

Understanding adsorption kinetics is critical for determining the appropriate settings for a large-scale batch operation. As a result, the Lagergren pseudo-first-order (PFO) model (Equation 7, Table 2) and Ho's pseudo-second-order (PSO) model (Equation 8, Table 2) were applied to explore the rate of MG adsorption onto PAOPT. Figure 6a-b shows the fits of the experimental findings to the specified models, and Table 3 shows the values of the calculated parameters as well as statistical constants. According to Lagergren's PFO model, low correlation coefficients are produced, R^2, with the highest χ^2 and RSS values. Ho's PSO model, on the other hand, is entirely appropriate to describe the kinetics of MG adsorption on the PAOPT, with a strong correlation coefficient (R^2) of 0.70 to 0.99 and low χ^2 and RSS values at different MG concentrations. Several researchers obtained similar MG adsorption kinetic results with other adsorbents [Ahmad Khan et al., 2023; Xu et al., 2023].

Furthermore, the adsorption capacity of PAOPT increased from 10.95 to 23.45 and 36.64 mg/g as the MG dye concentration rose from 5 to 10 and 20 mg/L, respectively, because greater MG molecules concentrations have a larger driving power, enabling them to break through the adsorbent-liquid mass transfer barrier. When MG concentrations are increased, the initial rate constants (k_2) decline from 0.20 to 0.18 and 0.058 g/mg.min, respectively. This implies that a faster interaction between MG molecules and the binding active sites had occurred at low dye concentrations.

Adsorption isotherm studies

At a fixed temperature, adsorption isotherms describe the process of retaining or releasing a substance from the water phase to the solid phase. They are crucial in understanding the adsorption capacity, the interaction between adsorbate and adsorbent surface characteristics, and the adsorption mechanism [Krishna Murthy et al., 2019]. To get the optimal equilibrium curves in this work, two-parameter isotherm models, namely Langmuir (Eq. 9) and Freundlich (Eq. 10) isotherm models, were applied. The Langmuir model depends on the assumption of monolayer homogenous adsorption, no contact between adsorbed molecules, and there are no discernible adsorption sites [Langmuir, 1918]. In contrast, the Freundlich equation assumes heterogeneous and multilayer adsorption [Freundlich, 1926]. Table 2 contains the mathematical equations and descriptions of the selected models' parameters.

Figure 7 shows the fits of the experimental isotherm findings to the models, and Table 4 summarises the calculated model parameters and statistical constants acquired from the two chosen isotherm

Table 3. Kinetic models' constants for PFO and PSO models for the MG adsorption on the PAOPT surface

Model	Pseudo–First Order (PFO)					Pseudo–Second Order (PSO)				
MG (mg/L)	q_e (mg/g)	k_1 (1/mim)	R^2	χ^2	RSS	q_e (mg/g)	k_2 (g/mg.min)	R^2	χ^2	RSS
5	10.95	1.03	0.35	0.25	2.78	11.27	0.20	0.70	0.12	1.27
10	23.45	1.30	0.41	0.16	3.64	23.81	0.18	0.73	0.07	1.66
20	36.64	0.98	0.44	0.72	26.43	37.70	0.058	0.99	0.31	10.82
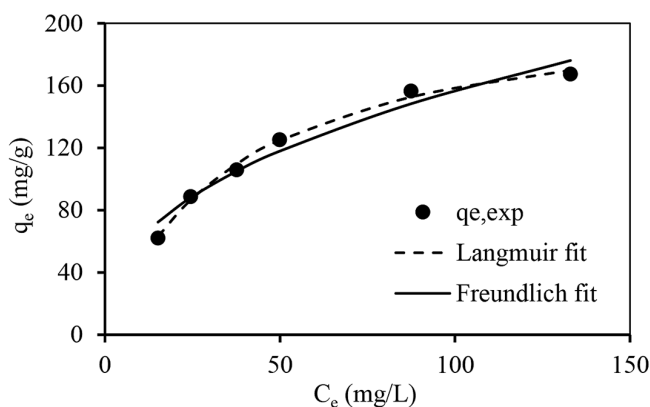
Figure 7. Langmuir and Freundlich isotherm plots for MG adsorption on PAOPT

Table 4. Langmuir and Freundlich isotherm constants and statistical constants of MG adsorption on PAOPT surface

Model	Constants				
Langmuir	q_m, (mg/g)	K_L, (1/min)	R^2	χ^2	RSS
	217.23	0.027	0.99	0.33	40.15
Freundlich	(mg/g)/(mg/L) ^{n}	n	R^2	χ^2	RSS
	23.75	0.41	0.97	2.81	302.8

models. According to the results shown in Figure 7 and Table 4, compared to the Freundlich isotherm model, R^2 value of 0.99 indicates a strong association between the Langmuir model calculated and experimental findings, which is supported by lower values of various statistical measures of χ^2 of 0.33 and RSS of 40.15. These findings indicated that MG adsorption happens mostly on the adsorbent's surface and that monolayer adsorption dominates the behaviour. Using an equivalent method, similar observations were reported by Krishna Murthy et al. (2019) and Xu et al. (2023).

Comparison of PAOPT performance with other adsorbents

Table 5 presents a comparison of the maximal adsorption capability of PAOPT with that of different adsorbents used for MG adsorption. When compared to other adsorbents, the PAOPT adsorption ability was considered high. Interestingly, PAOPT adsorbed MG from the liquid phase much faster

than in previous studies. As a result, PAOPT outperformed other adsorbents; therefore, PAOPT can be employed as an alternate adsorbent in removing low MG concentrations from watery liquids.

Desorption study

The proportion of desorption at a neutral medium using distilled water and an acidic one using 0.01 M HCl solution is shown in Table 6. Distilled water could not desorb MG from the loaded PAOPT (i.e. desorption percentage was zero), but the 0.01 M HCl desorption percentage was 19.65. This finding confirmed the robust contact between the MG and the PAOPT surface, consistent with the FTIR spectra. Furthermore, the low PAOPT desorption percentage using 0.01 M HCl revealed that MG had an electrostatic attraction with PAOPT besides additional strong interaction with the PAOPT surface, such as H-bonding and π-π interaction (not sensitive to ionic strength), which resists desorption and makes removal difficult.

Table 5. Assessment of PAOPT adsorption capability for MG with other adsorbents

Adsorbent	pH	Time	Temp. (K)	$q_{cal, max}$ (mg/g)	Reference
PAOPT	6	20	298	217.23	This study
Willow leaves powder (WLP)	NA	40	278	10.01	[Ahmad Khan et al., 2023]
Willow leaves biochar (WLB)				21.244	
Hydrochar from peanut shell (HC-PS)	NA	1440	NA	570.34	[Xu et al., 2023]
Hydrochar from pine (HC-PE)				562.2	
Nymphaea lotus (WLSAB)	7	30	301	102.35	[Jabar and Odusote, 2021]
Activated carbon of fig leaves	10	20	298	51.79	[Gebreslassie, 2020]
Acid treated Coffee husk (ACH)	6.8	120	303	195.34	[Krishna Murthy et al., 2019]
Cassava stem biochar (CSB)	7	10	NA	40.5	[Zaid et al., 2017]
Activated carbon of oil palm trunk fibre (OPTF)	5	115	303	149.35	[Hameed and El-Khaiary, 2008]
NA: Not available					

Table 6. The adsorption-desorption percentage using distilled water and 0.01 M HCl

Distilled water		0.01 M HCl	
Adsorption (%)	Desorption (%)	Adsorption (%)	Desorption (%)
75.84	0	76.09	19.65

CONCLUSIONS

An agricultural solid waste, oil palm trunk (OPT), was chemically treated with 0.10 M H_3PO_4 and used as a low-cost substitute adsorbent (PAOPT) for the elimination of harmful dyes such as MG. The chemical treatment successfully altered the physicochemical properties of PAOPT. Batch tests for the MG adsorption revealed that the adsorption ability of PAOPT towards MG improved as solution pH and contact time increased. It has been discovered that as PAOPT dosage increases, the MG removal percentage also increases. The maximum MG adsorption was attained at pH 6, 20 min, and 0.02 g of PAOPT adsorbent. The PAOPT adsorption kinetics were well-matched to the PSO model. The adsorption data best suited the Langmuir isotherm model with $R^2 = 0.99$, confirming that MG molecules were monolayer covered on the PAOPT surface. The PAOPT had a maximum adsorption capacity of 217.23 mg/g at pH 6 and 298 K. Based on the FTIR spectra and desorption investigations, electrostatic attraction and other interactions, including H-bonding and π-π interaction, performed a significant role in the PAOPT adsorption process. These findings show that PAOPT adsorbent can be a low-cost and readily available alternative for MG extraction from water-based solutions.

REFERENCES

1. Ab Aziz, N.A.H., Md Ali, U.F., Ahmad, A.A., Mohamed Dzahir, M.I.H., Khamidun, M.H. and Abdullah, M. F. 2023. Non-functionalised oil palm waste-derived reduced graphene oxide for methylene blue removal: Isotherm, kinetics, thermodynamics, and mass transfer mechanism. Arabian Journal of Chemistry, 16(1), 104387. https://doi.org/10.1016/j.arabjc.2022.104387

2. Abdul Khalil, H.P.S., Siti Alwani, M., Ridzuan, R., Kamarudin, H., Khairul, A. 2008. Chemical Composition, Morphological Characteristics, and Cell Wall Structure of Malaysian Oil Palm Fibers. Polymer-Plastics Technology and Engineering, 47, 273–280. http://doi.10.1080/03602550701866840

3. Ahmad Khan, F., Dar, B.A., Farooqui, M. 2023. Characterisation and adsorption of malachite green dye from aqueous solution onto *Salix alba* L. (Willow tree) leaves powder and its respective biochar. International Journal of Phytoremediation, 25(5), 646–657. https://doi.org/10.1080/15226514.2022.2098909

4. Freundlich, H. 1926. Colloid and Capillary Chemistry. Methuen, Lon.

5. Gebreslassie, Y.T. 2020. Equilibrium, Kinetics, and Thermodynamic Studies of Malachite Green Adsorption onto Fig (*Ficus cartia*) Leaves. Journal of Analytical Methods in Chemistry, 2020, https://doi.org/7384675.10.1155/2020/7384675

6. Hameed, B.H., El-Khaiary, M.I. 2008. Batch removal of malachite green from aqueous solutions by adsorption on oil palm trunk fibre: Equilibrium isotherms and kinetic studies. Journal of Hazardous Materials, 154(1), 237–244. https://doi.org/10.1016/j.jhazmat.2007.10.017

7. Harith Zafrul Fazry, A., Sapawe, N., Izhar Fahimi Abdul Aziz, A., Zafri Haiqal Zainudin, M., Hakimi Haizal Hafiz, M., Aiman Farhan Idris, M., Farhan Hanafi, M., Farhan Mohd Fozi, M. 2018. Microwave induced HNO_2 and H_3PO_4 activation of oil palm frond (OPF) for removal of malachite green. Materials Today: Proceedings, 5, (10, Part 2), 22143–22147. https://doi.org/10.1016/j.matpr.2018.07.082

8. Haroon, M., Ullah, R., Ullah, S., Mehmood, S., Khan, N., Haq, F., Uddin, W., Ullah, N., Ali, Z., Majeed, H. 2021. Efficient adsorption of Malachite Green from water by activated carbon of Date trunk fiber. Journal of Applied and Emerging Sciences, 11(1), 57–62.

9. Hasan, R., Ahliyasah, N.A.F., Chong, C.C., Jusoh, R., Setiabudi, H.D. 2019. Eggshell treated oil palm fronds (EG-OPF) as low-cost adsorbent for methylene blue removal. Bulletin of Chemical Reaction Engineering & Catalysis, 14(1), 158–164.

10. Ho, Y.-S., McKay, G. 1999. Pseudo-second order model for sorption processes. Process Biochem, 34(5), 451–465.

11. Husien, S., El-taweel, R.M., Salim, A.I., Fahim, I.S., Said, L.A., Radwan, A.G. 2022. Review of activated carbon adsorbent material for textile dyes removal: Preparation, and modelling. Current Research in Green and Sustainable Chemistry, 5, 100325. https://doi.org/10.1016/j.crgsc.2022.100325

12. Jabar, J.M., Odusote, Y.A. 2021. Utilisation of prepared activated biochar from water lily (*Nymphaea lotus*) stem for adsorption of malachite green dye from aqueous solution. Biomass Conversion and Biorefinery. https://doi.org/10.1007/s13399-021-01399-9

13. Jasri, K., Abdulhameed, A.S., Jawad, A.H., Alothman, Z.A., Yousef, T.A., Al Duaij, O.K. 2023. Mesoporous activated carbon produced from mixed wastes of oil palm frond and palm kernel shell using microwave radiation-assisted K_2CO_3 activation for methylene blue dye removal: Optimisation by response surface methodology. Diamond and Related Materials, 131, 109581. https://doi.org/10.1016/j.diamond.2022.109581

14. Khalid, K., Hanafiah, M.A.K.M., Al-Amrani, W.A., Nik Malek, N.A.N., Fatinathan, S. 2022. Comparative Adsorption of Methylene Blue Dye on Hexane-Washed and Xanthated Spent Grated Coconut (*Cocos nucifera* L.): Isotherms, Thermodynamics, and Mechanisms. Journal of Ecological Engineering, 23(3), 1-11. https://doi.org/10.12911/22998993/145675.

15. Krishna Murthy, T.P., Gowrishankar, B.S., Chandra Prabha, M.N., Kruthi, M., Hari Krishna, R. 2019. Studies on batch adsorptive removal of malachite green from synthetic wastewater using acid treated coffee husk: Equilibrium, kinetics and thermodynamic studies. Microchemical Journal, 146, 192–201. https://doi.org/10.1016/j.microc.2018.12.067.

16. Lagergren, S.K. 1898. About the theory of so-called adsorption of soluble substances. Sven Vetenskapsakad Handingar, 24, 1–39.

17. Lan, D., Zhu, H., Zhang, J., Li, S., Chen, Q., Wang, C., Wu, T., Xu, M. 2022. Adsorptive removal of organic dyes via porous materials for wastewater treatment in recent decades: A review on species, mechanisms and perspectives. Chemosphere, 293, 133464. https://doi.org/10.1016/j.chemosphere.2021.133464

18. Langmuir, I. 1918. The adsorption of gases on plane surfaces of glass, mica and platinum. Journal of American Chemical Society, 40, 1361–1403.

19. Lawal, A.A., Hassan, M.A., Ahmad Farid, M.A., Yasim-Anuar, T.A.T., Mohd Yusoff, M.Z., Zakaria, M.R., Roslan, A.M., Mokhtar, M.N., Shirai, Y. 2020. One-step steam pyrolysis for the production of mesoporous biochar from oil palm frond to effectively remove phenol in facultatively treated palm oil mill effluent. Environmental Technology & Innovation, 18, 100730. https://doi.org/10.1016/j.eti.2020.100730

20. Lim, A., Chew, J.J., Ismadji, S., Khaerudini, D.S., Darsono, N., Sunarso, J. 2022. Kinetic and equilibrium adsorption study of anionic dyes using oil palm trunk-derived activated carbon. Materials Today: Proceedings, 64, 1627–1638. https://doi.org/10.1016/j.matpr.2022.04.918

21. Miranda, F.F., Putri, A.S., Mustikaningrum, M., Yuliansyah, A.T. 2021. Preparation and characterisation of nano crystal cellulose from oil palm trunk for adsorption of methylene blue. AIP Conference Proceedings, AIP Publishing LLC.

22. Mustikaningrum, M., Cahyono, R.B., Yuliansyah, A.T. 2021. Effect of NaOH concentration in alkaline treatment process for producing nano crystal cellulose-based biosorbent for methylene blue. IOP Conference Series: Materials Science and Engineering, IOP Publishing.

23. N'diaye, AD., Kankou, M.S.A., Hammouti, B., Nandiyanto, A.B.D., Al Husaeni, D.F. 2022. A review of biomaterial as an adsorbent: From the bibliometric literature review, the definition of dyes and adsorbent, the adsorption phenomena and isotherm models, factors affecting the adsorption process, to the use of typha species waste as adsorbent. Communications in Science and Technology, 7(2), 140–153.

24. Ngaha, M.C.D., Njanja, E., Doungmo, G., Tamo Kamdem, A., Tonle, I.K. 2019. Indigo Carmine and 2,6-Dichlorophenolindophenol Removal Using Cetyltrimethylammonium Bromide-Modified Palm Oil Fiber: Adsorption Isotherms and Mass Transfer Kinetics. International Journal of Biomaterials, 2019, 6862825. https://doi.org/10.1155/2019/6862825.

25. Pereira, L., Alves, M. 2012. Chapter 4: Dyes-environmental impact and remediation. Environmental protection strategies for sustainable development, strategies for sustainability. A. Malik and E. Grohmann, Springer Science+Business Media BV: 111–162.

26. Xu, Y., Zhang, J., Jia, G., Ji, D., Ding, Y., Zhao, P. 2023. Evaluating malachite green removal from aqueous solution by hydroxyl enhanced hydrochar and biomass. Biomass Conversion and Biorefinery. https://doi.org/10.1007/s13399-022-03647-y

27. Zaid, M., Jamion, N., Omar, Q., Yong, S. 2017. Sorption of malachite green (MG) by cassava stem biochar (CSB) kinetic and isotherm studies. Journal of Fundamental and Applied Sciences, 9(6S), 273–287.